Thermochimica Acta 533 (2012) 39–45

Contents lists available at SciVerse ScienceDirect

Thermochimica Acta

journal homepage: www.elsevier.com/locate/tca

Examination of water phase transitions in Loblolly pine and cell wall components by differential scanning calorimetry

Samuel L. Zelinka[a,*], Michael J. Lambrecht[b], Samuel V. Glass[a], Alex C. Wiedenhoeft[a], Daniel J. Yelle[a]

[a] US Forest Service, Forest Products Laboratory, United States
[b] Department of Chemistry, University of Illinois, United States

ARTICLE INFO

Article history:
Received 26 October 2011
Received in revised form 5 January 2012
Accepted 19 January 2012
Available online 2 February 2012

Keywords:
Differential scanning calorimetry (DSC)
Wood
Cellulose
Wood–water relations
Thermodynamics
Sorption

ABSTRACT

This paper examines phase transformations of water in wood and isolated wood cell wall components using differential scanning calorimetry with the purpose of better understanding "Type II water" or "freezable bound water" that has been reported for cellulose and other hydrophilic polymers. Solid loblolly pine (*Pinus taeda*) milled pine, and holocellulose, cellulose, and lignin isolated from the same parent board were tested. For each sample preparation, the freezing and melting of water was examined at 10–20 different moisture contents. Only one freezing peak was observed for most sample preparations; in these cases, the phase transformation corresponded to the "Type I" or "free water" peak. The freezing and melting temperatures of this Type I peak depended on moisture content, and appreciable undercooling (−30 °C from bulk water) was observed at the lowest moisture contents. The isolated ball-milled cellulose exhibited a Type II peak, yet the Wiley-milled cellulose, from which the ball-milled cellulose was made, did not exhibit a Type II peak. When present, the Type II peak is consistent with the homogeneous nucleation temperature of bulk water. The results suggest that the detection of Type II or freezable bound water in wood may depend more on sample preparation than the chemical nature of the cell wall component in question; a point not discussed by previous researchers describing Type II water in hydrophilic polymers.

Published by Elsevier B.V.

1. Introduction

The interaction of water with wood can cause durability issues such as dimensional instability, splitting, checking, mold growth, wood decay or corrosion of embedded metals. Traditionally, theories of moisture in wood partition water into two forms: "bound water" that is held within the cell walls and "free water" that exists in the lumina of the cells. The maximum amount of bound water that the cell walls can hold is termed the fiber saturation point (FSP) and occurs around 30% MC (moisture content) for most wood species [1,2]. Many of the physical and mechanical properties of wood that depend upon moisture below FSP, such as strength, shrinkage, and electrical resistivity are constant above FSP or exhibit very slight changes [3]. Despite the importance of FSP on wood properties, many of moisture induced wood durability issues, such as mold growth or corrosion of embedded fasteners occur at wood moisture contents well below FSP.

Zelinka et al. [4] proposed a percolation model for ionic conduction in wood where the percolation threshold, which physically represents the amount of water required to form a path of ionically conducting water in wood was below FSP. The percolation threshold, 16% MC, was taken from radioactive tracer measurements performed by Lin [5], who found that endogenous mineral ions in wood only moved in the presence of an electric field if the moisture content was greater than or equal to 16% MC. Several other phenomena such as mold growth [6], corrosion of embedded metals [7], and longitudinal shrinkage [8], also exhibit a threshold or discontinuity below FSP around 15–20% MC, approximately the same MC as the percolation threshold. Since these phenomena require water, it is reasonable to think that there may be a third type of water that behaves like free water below FSP.

The percolation threshold is consistent with previous nuclear magnetic resonance (NMR) and differential scanning calorimetry (DSC) measurements of water in wood and cellulose that exhibit multiple types of water. Using NMR, researchers have observed water with three different relaxation times which they have classified as free water, bound water, and water with a relaxation time between bound water and free water [9–12]. Examining hardwoods, Almeida et al. observed this intermediate water appeared between 12–16% MC for sugar maple (*Acer saccharum*) and beech (*Fagus grandifolia*) [10]. Nakamura et al. [13] used DSC to

* Corresponding author at: Durability and Wood Protection, US Forest Service, Forest Products Laboratory, 1 Gifford Pinchot Drive, Madison, WI 53726, United States. Tel.: +1 608 231 9277.
E-mail address: szelinka@fs.fed.us (S.L. Zelinka).

0040-6031/$ – see front matter. Published by Elsevier B.V.
doi:10.1016/j.tca.2012.01.015

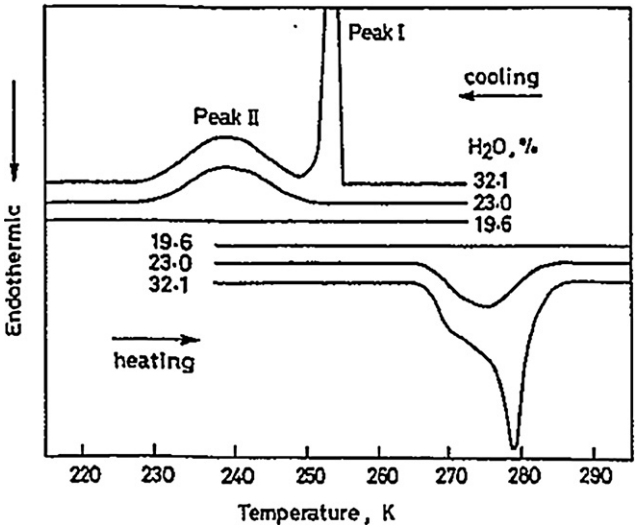

Fig. 1. Cellulose DSC curves presented by Nakamura et al. [6]. Reprinted with permission of Textile Research Journal.

examine water freezing in cellulose derived from wood and observed three distinct types of water. The DSC curves of Nakamura et al. are reprinted in Fig. 1 for reference. At low moisture contents, no exotherm was visible upon water freezing, and Nakamura et al. inferred that this water exists as traditional bound water. As the moisture content was increased, a thermal event was observed with a depressed freezing temperature (Peak II). At higher moisture contents, a thermal event occurred at the freezing temperature of water, and this thermal event is associated with free (unbound) water (Peak I). Peaks I and II coexisted over a range of moisture contents. Nakamura et al. referred to the water associated with Peak II as "freezable bound water". For clarity, we will refer to this water as "Type II" water as this parallels nomenclature used by other researchers who have argued that water in small pores gives rise to a Peak II in similar systems [14].

In further work, Hatakeyama et al. also observed Type II water in lignin extracted from *Calocedrus decurrens* [15]. What is especially interesting is the range of moisture contents over which Type II water appears; 12% for lignin and 12–24% for cellulose [13,15]. Other researchers have also observed two melting peaks in chemically modified cellulose [16]. As stated earlier, many moisture dependent wood properties also have threshold or discontinuous behavior in this moisture content range. In short, it is possible that the Type II water observed in lignin and cellulose may be responsible for processes in wood ranging from ionic conduction to corrosion of embedded metals.

Three previous papers examining the phase transition of water in solid wood have been published although the Type II water of Nakamura et al. has not been explicitly confirmed because these papers looked at the melting behavior only [17–19]. Despite only looking at melting curves, all three research groups inferred that two types of bound water might exist in wood. It is therefore instructive to contrast the physical picture of water in solid wood measured by these researchers with the "Type II" physical picture offered by Nakamura et al.

Simpson and Barton [17] examined the feasibility of using DSC as an accurate method to measure FSP for 3 species: *Eucalyptus marginata*, *Eucalyptus diversicolor*, and *Pinus radiata*. Specimens were 1–3 mm thick and 3 mm in diameter. The specimens were rapidly frozen to −22 °C and heated at a scan rate of 10 °C min^{-1} until the temperature was greater than 20 °C. A low temperature shoulder was observed on the melting peak, which was attributed to a type of water that was neither bound water nor free water.

Repellin and Guyonnet [19] used DSC to determine FSP in *Fagus sylvatica* and *Pinus pinaster* and compared the results to those obtained by volumetric shrinkage. Specimens, which weighed between 2 mg and 5 mg and were less than 1 mm thick, were rapidly frozen to −40 °C and brought to 40 °C at rate of 2 °C min^{-1}. Heating curves were run in wood that was well above fiber saturation; the area underneath the melting curve was attributed to free water. Using an assumed enthalpy of 334 J g^{-1}, the mass of melting water was determined, and the difference between this amount and the total amount of moisture in the sample gave their imputed FSP. Repellin and Guyonnet observed a "shoulder" on the melting peak which they attributed to water freezing in pores and used the Gibbs–Thompson equation to calculate the pore size.

Kärenlampi et al. [18] examined the phase transformations of water in 200 μm thick sections of spruce sapwood (*Picea* sp.) cut on a sliding microtome. The final samples weighed between 5 and 20 mg and were cooled to −45 °C at 10 °C min^{-1} before being returned to 25 °C at a rate of 5 °C per minute, although some of the specimens were held at −45 °C for 6 h to examine the effect of "time-dependent freezing". The authors invoke the concept of a type of water between bound and free water to explain a freezing point depression; however, it is unclear on what the authors base this, as no calorimograms were presented, freezing temperatures were not reported, and it is well known that bulk water frequently supercools to temperatures below −15 °C in DSC experiments for kinetic (not thermodynamic) reasons [20].

In summary, the literature on the phase transformations of water in solid wood invoke the concept of two types of bound water, which is consistent with Nakamura's observation of Type II water in cellulose. However, it needs to be emphasized that none of the previous wood research has demonstrated (or tested) the two peak freezing curve (i.e., Fig. 1), which was the basis for the partitioning of water into the three types proposed by Nakamura et al. [13]. We therefore sought to determine whether the Type II peak observed in cellulose also exists in solid wood, and if so, whether this Type II water may help explain durability problems that arise in wood below the fiber saturation point. This work explores phase transformations of water in solid wood and isolated wood cell wall components, with the goal of better understanding "Type II" water and identifying in which cell wall components Type II peaks can be found.

2. Experimental procedure

A top-down approach was taken to explore the effects of polymer structure on the freezing of water in loblolly pine (*Pinus taeda*). Solid, Wiley-milled (40 mesh), and ball-milled pine were examined, as were holocellulose, cellulose, and lignin. All material except the solid pine came from the same parent source, which contained only mature sapwood. Compositional analysis of the wood showed that it had a cellulose/hemicelluloses/lignin ratio of 45/22/33 and contained 9 wt% of extractives. The Wiley-milled and ball-milled pine were tested "as is" and after being exhaustively Soxhlet extracted. The different components and sample preparations are summarized in Table 1 for clarity. For each sample preparation, the freezing and melting of water was examined in 10–20 specimens at prepared to have different moisture contents. To ensure that the separate pieces of pine were similar, we Wiley-milled a portion of the solid pine to 40 mesh for comparison. Similar behavior between the two Wiley-milled woods tested suggested no apparent differences between these two sources of material (see Section 3 and Table 2).

The ball-milled wood (from a previous study [21]) and isolated cell wall components were prepared from a single piece of loblolly pine. The wood was Wiley-milled until it passed through a 40 mesh

Table 1
Summary of the sample preparations and cell wall components tested, along with the abbreviations and symbols used throughout the paper.

	Symbol	Preparation	Full description
WM pine	○	Wiley-milled (40 mesh)	Loblolly pine Wiley-milled to 40 mesh
BM Pine	●	Ball-milled	Loblolly pine Wiley-milled to 40 mesh and then vibratory ball-milled
WM(e) pine	□	Wiley-milled (40 mesh)	Loblolly pine Wiley-milled to 40 mesh and then exhaustively Soxhlet extracted
BM(e) pine	■	Ball-milled	Loblolly pine Wiley-milled to 40 mesh and then exhaustively Soxhlet extracted and then vibratory ball-milled
Solid pine	*	Cut from solid wood	Loblolly pine microtomed on 1 side and then cut to roughly 1 mm thick
Holocellulose	◊	Wiley-milled (40 mesh)	Holocellulose extracted from WM(e) Pine
Lignin	►	Ball-milled	Lignin prepared from BM(e) Pine
WM cellulose	△	Wiley-milled (40 mesh)	Cellulose extracted from Holocellulose
BM cellulose	▲	Ball-milled	Cellulose extracted from Holocellulose and then planetary ball-milled

Table 2
Results of linear least square fits of the enthalpy data.

Source	Material	Slope ($J\,g^{-1}$)	*X*-intercept (FSP)
Yelle et al. [21]	Lignin (►)	258	0.2
	WM cellulose (△)	208	0.26
	WM pine (○)	231	0.26
	Holocellulose (◊)	244	0.28
	WM(e) pine (□)	243	0.28
	BM cellulose (▲)	226	0.28
	BM Pine (●)	246	0.31
	BM(e) pine (■)	232	0.32
Average		**236**	
Wood collection	Solid wood (*)	226	0.27
	WM pine (not plotted)	232	0.26

filter. Half of this material was then exhaustively Soxhlet extracted sequentially through a series of the following solvents: distilled water, methanol, acetone, and chloroform. The extraction was carried out for 8 h with each solvent. Portions of the extracted and unextracted Wiley-milled wood were then placed in a vibratory ball mill. The ball milling was performed for 48 h with a repeating pattern of 30 min of vibration followed by 30 min of rest.

Lignin was isolated from the ball-milled wood using the method of Björkman [22] then lyophilized. Holocellulose was prepared from the extracted Wiley-milled wood using the method of Wise et al. [23] then lyophilized. Cellulose was prepared from the holocellulose fraction using a similar method to that of Capek et al. [24] then lyophilized. A portion (1 g) of this cellulose was then ball-milled in a Retsch (Newtown, PA) PM-100 planetary ball-mill equipped with a 50 mL ZrO_2 cup and ZrO_2 balls using the following parameters: 3 h with eight 10 mm balls plus three 20 mm balls, 600 rpm, 20 min interval, 10 min pause; 12 h with ten 10 mm balls, 600 rpm, 20 min interval, 10 min pause.

Solid wood samples were surfaced with a microtome on the transverse surface, 1 mm was cut from the end of the specimen with a precision micro-table saw, and this piece of wood was then split with a razor blade into sub-pieces small enough to fit in DSC sample pans. The solid wood was placed in the pan with the microtomed surfaces face-down to be in contact with the thermal transfer surface of the DSC.

All sample preparations (Table 1) were examined with light microscopy to quantify particle sizes and other features. Unfortunately, the ball-milled material was prone to clumping together which made it impossible to take a statistically meaningful measurement of the particle size distribution.

For all samples, care was taken to determine the mass as exactly as possible, as small changes in the mass could have a large effect on the calculated moisture content. All weighing was performed on either a thermogravimetric analyzer (TGA) or dynamic vapor sorption apparatus (DVS) that contained a balance with a precision of 0.1 μg. Samples were prepared by first weighing the DSC sample pan, lid, and hermetic seal. Afterward, water was added, and finally the wood material before being hermetically sealed. After it was sealed, the sample was allowed to sit for at least 24 h before testing to allow for water redistribution within the sample. The mass of the sample and pan was determined prior to testing in the DSC.

The cooling and heating curves were taken with Q200 and Q2000 DSCs (TA Instruments, New Castle, DE) with refrigerated cooling systems (RCS) capable of cooling to −90 °C. While −90 °C was the lower limit of the RCS, it was found that the cooling system could not keep up with the cooling rate below −70 °C, which caused a deviation in the baseline. After optimizing the scan rate and temperature profiles, the following protocol was chosen. The specimen was held isothermally at 25 °C for 5 min. The temperature was then decreased at 5 °C per minute until the specimen reached −65 °C, at which temperature it was held for an additional 5 min. The specimen was then heated at 5 °C per minute until the temperature reached 25 °C. The scan rate was chosen to match that used by Nakamura et al. [13] who observed two freezing peaks in cellulose.

After the DSC measurements were taken, a small hole was poked through the hermetic seal and the specimen was placed in an oven at 105 °C for several hours. After oven drying, the sample was transferred to the TGA or DVS where it was held at 105 °C until the change in mass was less than or equal to 0.0005% per minute (approximately 0.4 μg/min for an average sample). This mass was used to calculate the oven-dry mass for the purposes of calculating moisture content.

3. Results

The freezing behavior depended on whether the specimens had been Wiley-milled or ball-milled. For Wiley-milled specimens, the freezing temperature gradually increased with moisture content, leveling off around 36% MC, and only one peak was observed. For ball-milled specimens, the freezing onset temperature occurred either near −45 °C for low moisture contents or abruptly transitioned to near −20 °C (same as bulk water) at high moisture contents. To illustrate these behaviors, the freezing temperature as a function of moisture content is illustrated in (Fig. 2). In some cases, for ball-milled specimens, a clear peak was observable at −45 °C, and a broad, jagged peak occurred at higher temperatures, which we will refer to hereafter as a "pseudo-Type II" behavior (Fig. 3 left). The ball-milled cellulose clearly exhibited two freezing peaks (Fig. 3 right); notably, the Wiley-milled cellulose only exhibited one peak. For the ball-milled cellulose, only one peak occurred at low moisture contents, and as the moisture content increased, two peaks were observed. At high moisture contents (not shown) only 1 peak occurred. When the same sample was melting and refrozen, the freezing curve retained both peaks in the same location.

Examples of freezing and melting curves are shown in Fig. 4 for holocellulose; the behavior for the other cell wall components was similar. One thermal event was observed for all heating curves, regardless of the freezing behavior. Both the peak temperature (the

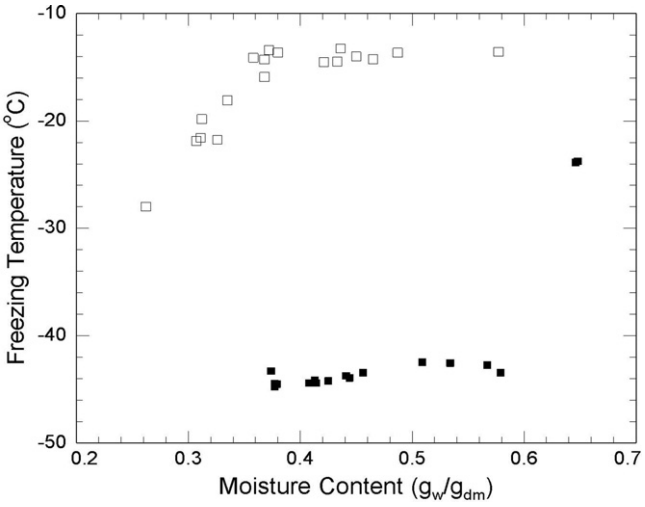

Fig. 2. Freezing temperature (onset) as a function of moisture content for WM(e) pine (□) and BM(e) pine (■). Other WM and BM specimens exhibited the same trends.

peaks were too broad to repeatedly measure onset temperature) of the thermal event and the enthalpy (area under the curve) varied with moisture content. The freezing phase transition occurs at a much lower temperature than the melting phase transition. This can be explained by kinetic supercooling upon freezing. However, the lowering of the phase transition temperature with moisture content appears to be a true thermodynamic undercooling as it appears in both freezing and melting and was found to be independent of scan rate (data not shown).

The melting enthalpy (normalized to the mass of dry wood), as a function of moisture content for all specimens tested, is shown in Fig. 5. The data are linear; the slope represents the enthalpy of melting of free water, and the intercept represents the point at which water ceases to freeze (i.e., the FSP). The data are bounded by lignin on the left (least hygroscopic) and the extracted ball-milled wood on the right (most hygroscopic). The slope and intercept of each curve are summarized in Table 2. It is clear that the enthalpies are lower than the enthalpy of pure water ($333\,J\,g^{-1}$). The nearly identical slope and intercept of the Wiley-milled pine from the wood collection and from Yelle et al. [21] suggests that the solid wood can be combined with the other data for analysis.

The melting temperature (measured at the peak) as a function of moisture content is shown in Fig. 6; the data are separated to highlight differences. In all cases, a large undercooling occurred at the lowest moisture contents to exhibit a melting endotherm. The peak temperature was used as opposed to the onset temperature because of the broadness of the peaks. For all components, besides the Wiley-milled and solid pine, there was a smooth transition across moisture contents and the asymptotic limit at high moisture contents was slightly lower than the melting temperature of bulk water. The trend appears similar for these groups; however, the data are spread out because there was a wide range of fiber saturation moisture contents for these groups. However, when the data were plotted so that the fiber saturation moisture content was zero (a shift in the *x* axis), the data were positioned on a single master curve (Fig. 6 inset). In contrast, the data for the solid and Wiley-milled pine displayed bilinear behavior. Moreover, the asymptote at high moisture contents sometimes occurred above the melting temperature of bulk water.

4. Discussion

The purpose of this work was to examine the freezing of water in wood and its cell wall components under a variety of preparation methods, and also to see if Type II water, which has already been observed in cellulose and lignin, exists in solid wood. The investigation yielded three major results: (1) the difference between cell wall constituents in the enthalpy/moisture content relation (Fig. 5), (2) the thermodynamic undercooling of the water melting temperature (Fig. 6), and (3) the presence and behavior of Type II water for certain sample preparations (Fig. 3). These results will be discussed in this order.

The slope of the melting enthalpy as a function of moisture content across all samples was constant at $240\,J\,g^{-1}$. The independence of cell wall component and preparation and slope suggests that the water undergoing the phase transformation is not interacting with the sample and we attribute the phase transition to the melting of free water in the samples. This independence may seem surprising given that cell wall components are believed to have large differences in the way they interact with water [2]. However, the constant slope between components suggests that the characteristics of free (unbound) water is the same for all cell wall components. Likewise, no differences were found in the melting enthalpy in the pine as the wood structure was removed in a series of steps from solid pine to WM-pine to BM-pine. From these measurements it appears the thermodynamics of free water are not affected by the location within the wood. The measured enthalpy ($240\,J\,g^{-1}$) was appreciably less than that of bulk water ($333\,J\,g^{-1}$). One possible explanation for this is that part of the melting enthalpy is buffered by the heat capacity of the remainder of the sample that does not freeze. A practical implication of this finding is that when DSC is used to investigate FSP, it is not sufficient to take a single measurement at saturation (and an assumed slope of $333\,J\,g^{-1}$) to calculate

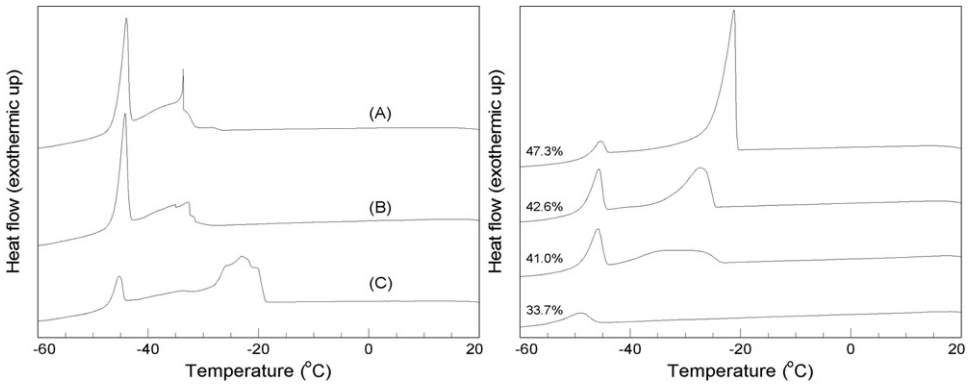

Fig. 3. Left: freezing curves exhibiting "pseudo-Type II peaks" (A) BM Pine (52.3% MC) (B) BM(e) Pine (50.9% MC) (C) BM(e) Pine (45.6% MC) Right: BM cellulose clearly exhibiting Type II peak, labeled with the % MC.

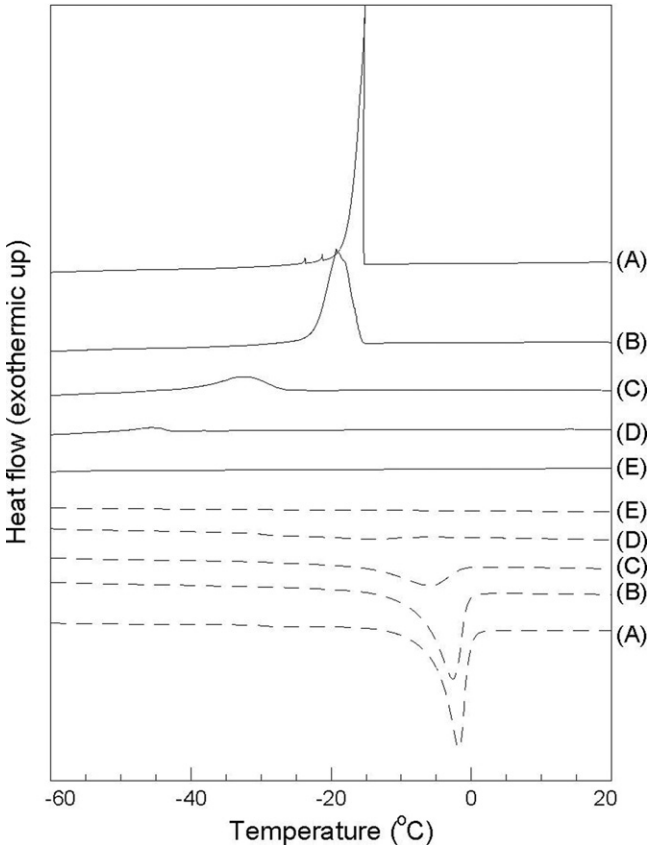

Fig. 4. DSC freezing (solid) and melting (dashed) curves for holocellulose as a function of moisture content: (A) 68% (B) 54.4% (C) 39.6% (D) 28.3% (E) 21.7%.

FSP, as has been done previously [19] as this will lead to an overestimation of FSP.

The extrapolation of the enthalpy as a function of moisture content to the ordinate axis represents the moisture content at which free water first appears – or FSP. Since the apparent FSP depends on the method used to determine it, it is worthwhile to place the enthalpy extrapolation in the context of other methods used to measure FSP. Several researchers [3,25,26] have noted that the pressure plate and polymer exclusion methods gave much higher values for FSP than methods based upon extrapolating physical properties that change below FSP but are nearly constant above

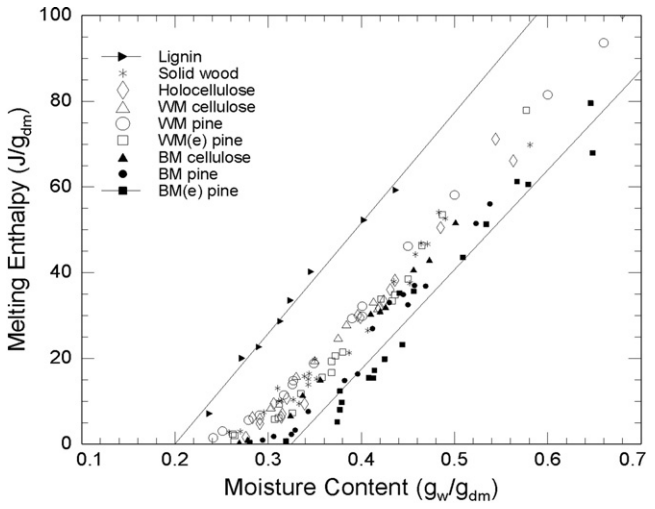

Fig. 5. Melting enthalpy as a function of moisture content.

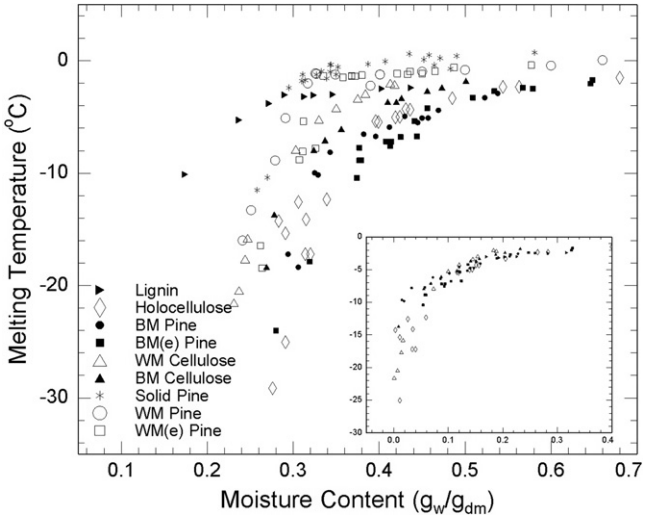

Fig. 6. Melting temperature as a function of moisture content. Inset: data shifted along the *x*-axis as moisture content above fiber saturation for lignin, holocellulose, BM Pine, BM(e) Pine, WM Cellulose and BM Cellulose.

FSP, such as electrical resistivity or shrinkage. While the enthalpy extrapolation is similar to other physical property extrapolations it is unique in that the property changes in the overhygroscopic region and it is extrapolated to low MC. Interestingly, the range of measured FSPs is similar to FSPs measured by extrapolation of other properties from the hygroscopic region [3].

Where a sample was tested in both the Wiley-milled and ball-milled states, the ball-milled specimens have a higher FSP. That is, the ball-milled specimen was able to bind more water within the polymer before saturation was reached when compared to a Wiley-milled specimen. Likewise, where a Wiley-milled specimen was tested in both extracted and unextracted states, the extracted specimen had a higher FSP, although this effect was smaller in ball-milled specimens. Lignin, known to be the least hydrophilic of the wood polymers had the lowest FSP. Cellulose and holocellulose had similar FSP values as the solid pine. While it is not surprising that cellulose and solid pine could hold more water than lignin, the data do highlight the effects of sample preparation. Specifically, it appears that ball-milling not only creates smaller particle sizes, but also exposes more hydrophilic functional groups on the polymers so that they are able to hold more water through hydrogen bonding.

All samples exhibited thermodynamic undercooling of the melting temperature, in some cases as much as 30 °C. The melting temperature depended on the total moisture content of the specimen, and approached the melting temperature of free water (0 °C) as the specimen moisture content increased. This large undercooling has been observed in other biologically-derived substances that interact with water such as processed cheese spreads [27] and milk [28]. In these systems, undercooling was described in terms of solution thermodynamics. Solution thermodynamic models included a eutectic phase transformation to account for the undercooling.

Although similar to these food substances, the interaction of wood and cellulose with water are traditionally fit only in the hygroscopic region with sorption models (such as the BET [29] or GAB [30] isotherm) as opposed to solution models. One possibility for the difference in models used to describe water interacting with these substances is that wood has a solid structure that can accommodate water, whereas milk is mostly water and approaches a solid (cheese) from the liquid state. Likewise, the maximum moisture content for solid wood is roughly 60 wt% water (or 150% moisture content), and is determined by the amount of empty space in the structure [31], and therefore, it is awkward to discuss “dissolving”

wood into water. Most wood-water research has been focused on the thermodynamics of going from 0 wt% water to ~30 wt% water. In such regimes, sorption models are able to fit this behavior well, although physical parameters derived from these models, such as the heat of sorption, do not agree with the observed behavior [32]. Because our melting temperature as a function of moisture content above FSP is so similar to those found by food researchers, and is described well by solution thermodynamics, it may be advantageous to transfer these models to wood.

One of the major objectives of this research was to better understand the Type II water reported from DSC measurements on lignin [15] and cellulose [13] and to see if this behavior could be confirmed in wood. While the calorimograms did not show Type II water for solid wood, the data illustrate the importance of sample preparation on the presence or absence of Type II water. This is most easily understood by comparing the two cellulose samples. The Wiley-milled cellulose did not Exhibit 2 peaks upon freezing, however, the ball-milled cellulose (which was further milled from Wiley-milled cellulose) clearly exhibited two peaks.

There has been discussion in the literature on whether the Type II peak was caused by water in small pores within the polymer structure [33–35], or was caused by water that was bound less tightly to the polymer and therefore had a different enthalpy [13,15,36–38]. It is interesting to examine this discussion in light of our observations that the presence or absence of the Type II peak is determined by sample preparation. The Wiley-milled cellulose consisted of large particles that retained some of the native wood structure whereas the ball-milled cellulose was likely completely amorphous [39]. If the Type II peak were caused by water freezing in small pores, we would expect to see observe the Type II peak in the preparations that had a porous structure, such as solid pine, or Wiley-milled pine. In fact, we observed the opposite, where the Type II water was only observed in ball-milled substances. Furthermore, if the freezing point were depressed because of the pore-size, we would expect a corresponding pore-melting peak. Landry examined the freezing of water in small pores using glass capillaries and a very slow scan rate ($0.05\,^{\circ}C\,min^{-1}$) and confirmed pore-melting behavior [20]. The scan rates used in this work and previous work on cellulosic materials were likely too fast to observe this phenomenon, however it should be noted the melting behavior of the Wiley-milled cellulose (one freezing peak) and ball-milled cellulose (two freezing peaks) were nearly identical (Fig. 6). Neither do our results suggest that the Type II peak is related to loosely bound water because the melting enthalpy of both Wiley-milled cellulose and ball-milled cellulose are linear with a similar slope (Fig. 5). If the Type II peak were related to loosely bound water, this water should have a different melting enthalpy as well. We believe that Type II water is neither a result of pore water or loosely bound water, but can instead be explained by nucleation kinetics.

In theory, water can be supercooled to $-38\,^{\circ}C$ before homogeneous nucleation spontaneously occurs [40]. However, in practice, water freezes near the thermodynamic melting temperature because of heterogeneous nucleation sites; that is, sites where the activation barrier of crystallization is lowered, such as container walls, chemical impurities, or dust particles [41]. Since only one nucleation site is needed to crystallize an entire liquid body, and even in high-purity liquids it has been estimated there are on the order of 10^{12} heterogeneous nucleation sites per cubic meter [41], homogeneous nucleation of liquids is rarely observed. Conversely, since melting does not involve nucleation, the melting reaction nearly always occurs at the equilibrium solidus temperature. Importantly, state variables, such as enthalpy, do not depend on whether the liquid-to-solid phase transformation occurs via homogeneous nucleation or heterogeneous nucleation.

We forward the following working hypothesis: "Type II" freezing peaks in our experiments are a result of homogeneous nucleation of water that is unconnected to the water that crystallizes at a higher temperature. The following facts are consistent with this hypothesis: (1) although sometimes two peaks are observed upon freezing, there is always only one melting peak; (2) where there are two peaks, the lower temperature peak always occurs near the homogeneous nucleation temperature of water; (3) the melting enthalpy is linear, the slope is nearly constant across specimens, and does not depend on how many freezing peaks were exhibited. This hypothesis is also consistent with the "pseudo-Type II" peaks exhibited by other ball-milled specimens in which some water had frozen before a clear, final freezing below $-40\,^{\circ}C$.

While our data suggest that Type II water may result from homogeneous nucleation in water that is not connected to the water that freezes heterogeneously, it is not clear why only the ball-milled specimens exhibit this peak since the ball-milled particles have lost the structure that is inherent in the solid and Wiley-milled wood. If the Type II water needs to be physically separated from the Type I water (which presumably nucleates heterogeneously) then we would expect the opposite results; namely that the micro- or submicroscopic structure of the wood cell wall provide the separation to permit the presence of two disparate types of water. To better understand the relationship between specimen characteristics and Type II water, future experiments should explore the role of particle size and chemistry on the presence/absence of Type II water.

One of our objectives was to relate the presence of Type II water to durability problems that arise in wood below the fiber saturation point. We found however, that the second freezing peak in the DSC measurements was sensitive to sample preparation and appears to be a result of homogeneous nucleation rather than a type of water with properties between bound and free water. Nevertheless, these experiments do not rule out the existence of an intermediate type of water that has been observed by NMR and that would be consistent with a threshold for electrical conduction, mold growth, and corrosion of metal fasteners, which all occur below FSP.

5. Summary and conclusions

The top-down approach used in this study to examine the freezing of water in solid wood and wood cell wall components clearly highlights the role of sample preparation for DSC measurements of water interacting with cellulose and other cell wall components. Not only did ball-milled specimens have a higher FSP, ball milling clearly affected the freezing behavior, and homogeneous nucleation was inferred from a Type II peak.

The melting temperature of the free water peak depended on moisture content. It may be possible from these data to construct a binary phase diagram for water in wood. Whereas sorption theories can only explain the thermodynamics of water below FSP, a phase diagram would extend the thermodynamic framework from ovendry wood, to 100% water.

Acknowledgements

The authors acknowledge funding from the U.S. Federal Highway Administration under the Cooperative Research Program for Covered Bridges. This article was written and prepared by US Government employees on official time, and it is therefore in the public domain and not subject to copyright. This article was improved by critical comments from two anonymous reviewers.

References

[1] S.L. Berry, M.L. Roderick, Plant–water relations and the fibre saturation point, New Phytologist 168 (2005) 25–37.
[2] C. Skaar, Wood–Water Relations, Springer-Verlag, New York, 1988.
[3] A.J. Stamm, Review of nine methods for determining the fiber saturation points of wood and wood products, Wood Science 4 (1971) 114–128.

[4] S. Zelinka, S. Glass, D. Stone, A percolation model for electrical conduction in wood with implications for wood–water relations, Wood and Fiber Science 40 (2008) 544–552.
[5] R.T. Lin, A Study of Electrical Conduction in Wood, State College of Forestry at Syracuse University, 1965.
[6] H. Viitanen, A.C. Ritschkoff, Mould growth in pine and spruce sapwood in relation to air humidity and temperature. Report No. 221, in, Swedish University of Agricultural Sciences, Department of Forest Products, 1991.
[7] N.R. Short, J.K. Dennis, Corrosion resistance of zinc-alloy coated steel in construction industry environments, Transactions of the Institute of Metal Finishing 75 (1997) 47–52.
[8] D.E. Kretschmann, S.M. Cramer, The role of earlywood and latewood properties on dimensional stability of loblolly pine, in: The Compromised Wood Workshop, Christchurch, New Zealand, 2007.
[9] J. Cox, P.J. McDonald, B.A. Gardiner, A study of water exchange in wood by means of 2D NMR relaxation correlation and exchange, Holzforschung 64 (2010) 259–266.
[10] G. Almeida, S. Gagne, R. Hernández, A NMR study of water distribution in hardwoods at several equilibrium moisture contents, Wood Science and Technology 41 (2007) 293–307.
[11] L. Thygesen, T. Elder, Moisture in untreated, acetylated, and furfurylated norway spruce studied during drying using time domain NMR1, Wood and Fiber Science 40 (2008) 309–320.
[12] L. Thygesen, T. Elder, Moisture in untreated, acetylated, and furfurylated norway spruce monitored during drying below fiber saturation using time domain NMR, Wood and Fiber Science 41 (2009) 194–200.
[13] K. Nakamura, T. Hatakeyama, H. Hatakeyama, Studies on bound water of cellulose by differential scanning calorimetry, Textile Research Journal 51 (1981) 607–613.
[14] S. Park, R.A. Venditti, H. Jameel, J.J. Pawlak, Changes in pore size distribution during the drying of cellulose fibers as measured by differential scanning calorimetry, Carbohydrate Polymers 66 (2006) 97–103.
[15] T. Hatakeyama, S. Hirose, H. Hatakeyama, Differential scanning calorimetric studies on bound water in 1,4-dioxane acidolysis lignin, Die Makromolekulare Chemie 184 (1983) 1265–1274.
[16] J. Berthold, J. Desbrières, M. Rinaudo, L. Salmén, Types of adsorbed water in relation to the ionic groups and their counter-ions for some cellulose derivatives, Polymer 35 (1994) 5729–5736.
[17] L.A. Simpson, A.F.M. Barton, Determination of the fibre saturation point in whole wood using differential scanning calorimetry, Wood Science and Technology 25 (1991) 301–308.
[18] P.P. Kärenlampi, P. Tynjälä, P. Ström, Phase transformations of wood cell water, Journal of Wood Science 51 (2005) 118–123.
[19] V. Repellin, R. Guyonnet, Evaluation of heat-treated wood swelling by differential scanning calorimetry in relation to chemical composition, Holzforschung 59 (2005) 28–34.
[20] M.R. Landry, Thermoporometry by differential scanning calorimetry: experimental considerations and applications, Thermochimica Acta 433 (2005) 27–50.
[21] D.J. Yelle, J. Ralph, C.R. Frihart, Characterization of nonderivatized plant cell walls using high-resolution solution-state NMR spectroscopy, Magnetic Resonance in Chemistry 46 (2008) 508–517.
[22] A. Björkman, Studies on finely divided wood. Part 1. Extraction of lignin with neutral solvents, Svensk Papperstidning 59 (1956) 477–485.
[23] L.E. Wise, M. Murphy, A.A. D'Addieco, Analyses of cellulose, Paper Trade Journal 122 (1946) 35.
[24] P. Capek, M. Kubacková, J. Alföldi, L. Bilisics, D. Lisková, D. Kákoniová, Galactoglucomannan from the secondary cell wall of *Picea abies* L. Karst, Carbohydrate Research 329 (2000) 635–645.
[25] C.A.S. Hill, The reduction in the fibre saturation point of wood due to chemical modification using anhydride reagents: a reappraisal, Holzforschung 62 (2008) 423–428.
[26] P. Hoffmeyer, E.T. Engelund, L.G. Thygesen, Equilibrium moisture content (EMC) in Norway spruce during the first and second desorptions, Holzforschung 65 (2011) 875–882.
[27] H. Gliguem, D. Ghorbel, C. Grabielle-Madelmont, B. Goldschmidt, S. Lesieur, H. Attia, M. Ollivon, P. Lesieur, Water behaviour in processed cheese spreads, Journal of Thermal Analysis and Calorimetry 98 (2009) 73–82.
[28] G. Vuataz, The phase diagram of milk: a new tool for optimizing the drying process, Lait 82 (2002) 485–500.
[29] S. Brunauer, P.H. Emmett, E. Teller, Adsorption of gases in multimolecular layers, Journal of the American Chemical Society 60 (1938) 309–319.
[30] R.B. Anderson, Modifications of the Brunaeur, Emmett, and Teller equation, Journal of the American Chemical Society 68 (1946) 686–691.
[31] S.V. Glass, S.L. Zelinka, in: R.J. Ross (Ed.), Moisture Relations and Physical Properties of Wood, U.S. Department of Agriculture, Forest Service, Forest Products Laboratory, 2010.
[32] W. Simpson, Sorption theories applied to wood, Wood and Fiber Science 12 (1980) 183–195.
[33] S. Deodhar, P. Luner, Measurement of Bound (Nonfreezing) Water by Differential Scanning Calorimetry, American Chemical Society, Washington, DC, 1980, pp. 273–286.
[34] Z.H. Ping, Q.T. Nguyen, S.M. Chen, J.Q. Zhou, Y.D. Ding, States of water in different hydrophilic polymers—DSC and FTIR studies, Polymer 42 (2001) 8461–8467.
[35] S. Park, R.A. Venditti, H. Jameel, J.J. Pawlak, Hard-to-remove water in cellulose fibers characterized by thermal analysis: a model for the drying of wood based fibers, Tappi Journal 6 (2007) 10–16.
[36] H. Hatakeyama, K. Nakamura, T. Hatakeyama, Studies on factors affecting the molecular motion of lignin and lignin-related polystyrene derivatives, Pulp and Paper Magazine of Canada 6 (1980) TR105–TR110.
[37] K. Nakamura, T. Hatakeyama, H. Hatakeyama, Relationship between hydrogen bonding and bound water in polyhydroxystyrene derivatives, Polymer 24 (1983) 871–876.
[38] H. Hatakeyama, T. Hatakeyama, Interaction between water and hydrophilic polymers, Themochimica Acta 308 (1998) 3–22.
[39] N. Stubicar, I. Smit, M. Stubicar, A. Tonejc, A. Janosi, J. Schurz, P. Zipper, An X-ray diffraction study of the crystalline to amorphous phase change in cellulose during high-energy dry ball milling, Holzforschung 52 (1998) 455–458.
[40] O. Mishima, H.E. Stanley, The relationship between liquid, supercooled and glassy water, Nature 396 (1998) 329–335.
[41] J.H. Perepezko, Nucleation kinetics and grain refinement, in: ASM Handbook vol. 15, Casting, ASM, International, Materials Park, OH, 2008, pp. 276–287.